Anal. Methods Environ. Chem. J. 8 (4) (2025) 97-110

AMECJ

Research Article, Issue 4
Analytical Methods in Environmental Chemistry Journal
Journal home page: www.amecj.com/ir

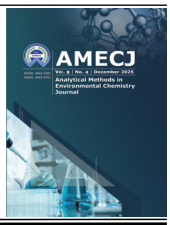

Efficient removal of methylene blue based on activated carbon derived from Pumpkin seed before analysis by UV-Vis spectroscopy

Ahmed S. Al-Rawi[a,*], Homam T. S. AL-Sayd Toohi[b], Abdulsalam M. Aljumialy[c], and Tahseen A. Zaidan[d]

[a]*Department of Chemistry, College of Science, University of Anbar, Ramadi 31001, Iraq*
[b]*Directorate of Education in Nineveh 41002, Iraq*
[c]*Department of Applied Chemistry, College of Applied Science, University of Fallujah, Fallujah 31002, Iraq*
[d]*Department of Applied Chemistry, College of Applied Sciences-Hit, University of Anbar, Hit 31007, Iraq*

ARTICLE INFO:

Received 16 July 2025
Revised form 25 Sep 2025
Accepted 3 Nov 2025
Available online 26 Dec 2025

Keywords:
Activated carbon;
Adsorption isotherms,
Biomass,
Dye,
UV-Vis spectroscopy

ABSTRACT

This study explores the utilization of pumpkin seeds as an abundant biomass resource and carbon precursor for the production of activated carbons. The precursor was activated at a 1:1.5 w/w ratio of pumpkin seeds to KOH at 650 °C to produce the activated carbons. SEM-EDX was used to observe the surface morphologies and compositions of the prepared activated carbons, which exhibit a clear porous surface structure and irregularly shaped particles. The activated carbons were used to remove methylene blue dye from aqueous solutions. The methylene blue concentration was determined using a UV-Vis spectrophotometer with a standard curve ranging from 5 to 25 mg L^{-1}, and the limit of detection and limit of quantification were 0.1027 and 0.3424 mg L^{-1}, respectively. A dosage of 0.05 g of activated carbon was sufficient to effectively remove more than 80% of the methylene blue within 5.0 min. The removal of methylene blue increases with contact time, reaching a maximum of 90% at 25 min. The removal of methylene blue is not affected by increasing temperature, but it is influenced by pH, with removal increasing as the medium becomes more alkaline. The adsorption isotherms show that the Freundlich and Temkin isotherms do not apply to the adsorption of the methylene blue onto the activated carbons. Still, the data fit well with the Langmuir isotherm model, which exhibits a high R^2 value (0.998).

1. Introduction

Pollution is one of the world's most critical and intractable problems. Due to industrial growth, pollution has become more detrimental to the environment than the usual standards that keep it in balance. As pollution levels continue to rise, the situation becomes more precarious, and the successful completion of substantial processing must comply with an increasing number of requirements [1–4]. Water pollution is among the most dangerous types of pollution, as water plays an essential role in maintaining life [5,6]. While the level of clean water is decreasing, it is important to find techniques to treat wastewater. A variety of studies seek suitable methods to conserve water reservoirs [7–9]. The most popular techniques for removing dyes from wastewater are the redox process [10–13] and adsorption methods [14,15] However, adsorption using carbon materials, such as activated carbon, is low-cost, easy, and environmentally friendly [16–18].

*Corresponding Author: Ahmed S. Al-Rawi
Email:ahmedeaheea@uoanbar.edu.iq
https://doi.org/10.24200/amecj.v8.i04.1071

Adsorption techniques using porous materials have been widely used for water treatment due to their ability to capture pollutants within their pores, achieving high removal efficiency. Natural clay, limestone, and dolomite, which are readily available, have been used to remove heavy metals from water [19–21]. Other porous materials, such as mesoporous silica composite with iron oxide and magnesium oxide, for the removal of methylene blue and lead and cadmium, respectively [7, 22, 23]. Cellulose acetate nanoparticles are used for the removal of salt from water [24]. Activated carbons have been widely reported as adsorbents due to their large specific surface area, high adsorption capacity, good surface activity, fine porous structure, and reactivity [25–30] Therefore, it is used in water treatment (removal of heavy metals and sulfur), adsorption of gases causing environmental pollution, and recovery of solvents used in industrial processes [31–35]. Evaluation of the amino acid concentrations in pumpkin seeds showed that arginine-glutamic and aspartic acids are the most critical residues, but tryptophan and methionine are the least important [36–38].That means this precursor is a good source of carbon, and the amino acid functional groups can enhance absorption. Pumpkin seeds are a side product with low cost and can be turned into a valuable product used to treat polluted water. This research aims to convert redundant Pumpkin seed products into valuable, economically feasible ACs and to investigate the potential of ACs as dye removers. Methylene blue was used as a model, and adsorption isotherms and thermodynamic parameters were used to study the adsorption conditions.

2. Experimental and Methods

2.1. Reagent

All chemicals and reagents, potassium hydroxide (CAS: 1310-58-3), hydrochloric acid (CAS: 7647-01-0), and methylene blue (CAS: 61-73-4), were obtained from Sigma-Aldrich. The methylene blue dye stock solution (1000 mg L^{-1}) was prepared by dissolving 1.0 g of methylene blue dye powder in double-distilled water. This solution was then used to prepare the required MB dye concentrations.

2.2. Preparation of ACs

Pumpkin seeds were mixed with KOH at a 1:1.5 (w/w) ratio and then thermally carbonized for 2

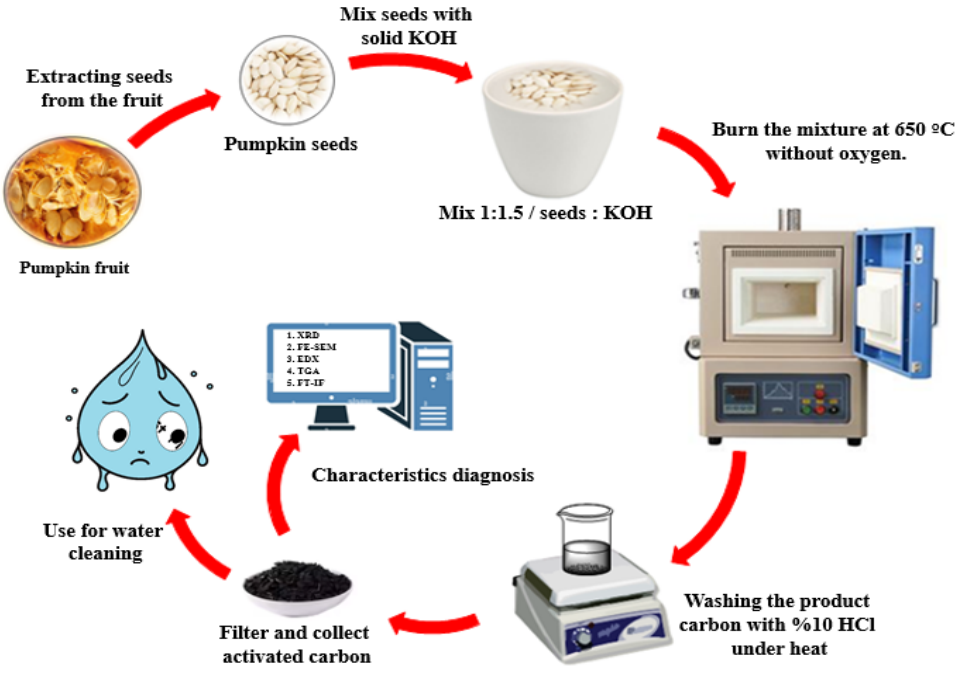

Fig. 1. Preparation and characterisation of ACs

hours in a furnace. This process was achieved by gradually increasing the temperature from 25 °C to 410 °C for 1 hour, then to 650 °C for 1 hour. The produced material was stirred with 10% HCl to remove residual KOH activation agent, metallic components, and contaminants. The sample was then filtered and washed with distilled water until the pH reached neutrality.

2.3. Characterization of ACs

The surface morphology of the ACs was investigated using a Scanning Electron Microscope (SEM) with Energy-Dispersive X-ray Spectroscopy (EDX). The composition of the ACs surface was analyzed by Field Emission Gun Scanning Electron Microscopy (Quanta 650 FEG-SEM). Water content and thermal stability of ACs at high temperatures were monitored by thermogravimetric analysis (TGA) and differential scanning calorimetry (DSC) under a nitrogen flow of 100 mL min^{-1}. The heating rate was 10 °C/min over the temperature range of 25 °C to 850 °C.

2.4. Adsorption process

We used the spectrophotometric method with a maximum wavelength between 200 nm and 800 nm to estimate the concentration of the MB in the aqueous solution using spectrophotometer (RAYLEIGH ,UV-1800) made in China. The λ_{max} of the MB dye was measured at 664 nm using the Beer-Lambert law (Equation 1).

$$A = \varepsilon\, b\, C \quad \text{(Eq.1)}$$

Where: A is absorbance; Ɛ is the molar absorption coefficient ($mol^{-1}.cm^{-1}$); b is the length of the light path (1 cm), and C is the molar concentration (mol L^{-1}). The adsorbent percentage was calculated using Equation 2, and the adsorption capacity was calculated using Equation 3.

$$\%\ \text{Adsorption} = \frac{C_i - C_e}{C_i} \times 100 \quad \text{(Eq. 2)}$$

$$q_e = \frac{C_i - C_e}{m} \times V \quad \text{(Eq. 3)}$$

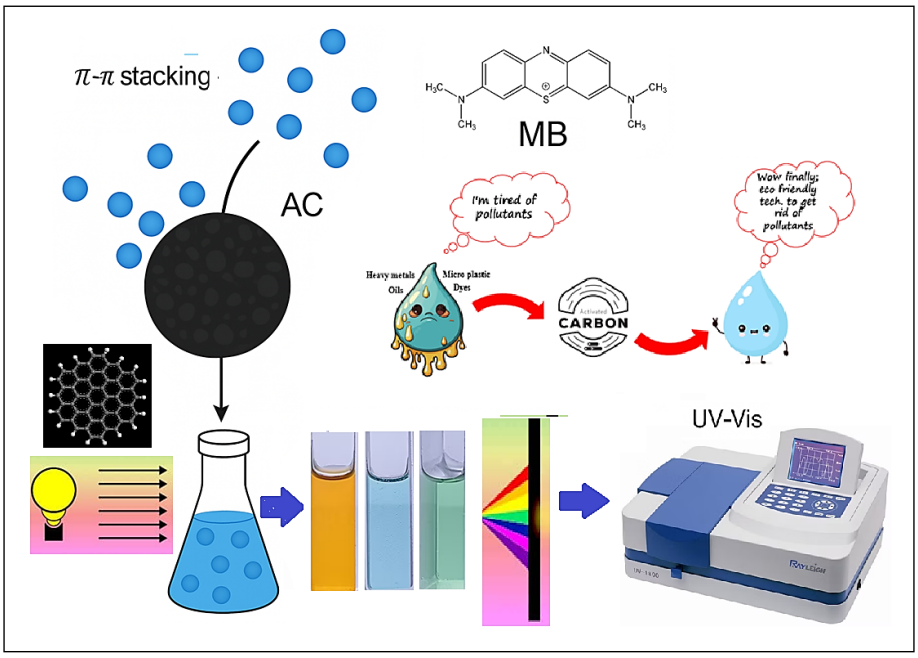

Fig. 2. Removal of pollutants with AC

Where C_i is the initial concentration, C_e is the concentration of residue in solutions (mg L^{-1}), m is the mass of the AC (g), and V is the volume of solution per liter.

The effect of AC dose was investigated by shaking 0.01, 0.02, 0.04, and 0.06 g of ACs with 100 mg L^{-1} of MB dye at 293 K for 5.0 min. The effect of contact time was determined by mixing 0.05 g of ACs with 100 mL of the dye (20 mg L^{-1}) at 293 ^oK for 5, 10, 15, 20, 25, and 30 minutes. To study the effect of initial concentration, an aqueous solution of MB dye was prepared in different concentrations (5, 10, 15, 20, and 30 mg L^{-1}). 0.05 g of AC was added to 100 mL of each concentration. The solutions were shaken (650 rpm min^{-1}) for 5 minutes. The solutions were then filtered, and the adsorption capacity and adsorption percentage were calculated. The effect of temperature was studied by shaking 100 mL of MB at 20 mg L^{-1} with 0.05g of AC at temperatures between 293 and 333 K. The solutions were shaken (650 rpm per min) for 5.0 minutes and then filtered, and the adsorption capacity and adsorption percentage were calculated.

3. Results and discussion

3.1. Nature and structure of AC

Numerous attempts have been performed to convert materials with high carbon content to activated carbon at various temperatures, which routinely reached more than 650 °C [35]. However, the pumpkin seeds were carbonized with KOH (1:1.5 w/w) at only 650 °C to obtain high-porous activated carbon, which is essential given the additional energy required. This might be related to the high amino acid content found in the pumpkin seed composition[37]. As the amino acids are easy to crash [39], activation with KOH could reduce the final carbonization temperature required for these materials. Previous studies have demonstrated an adverse relationship between the porosity of activated carbon and its density, accompanied by a positive correlation with surface area[40].

Figure 3A-3D presents the SEM-EDX analysis to visualize the morphology of ACs. The exterior surface structure of ACs appearing in Figure 1(a) was noticeably porous with irregularly shaped carbon. Pore formation can be attributed to the melting of the activator (KOH) on the biomass

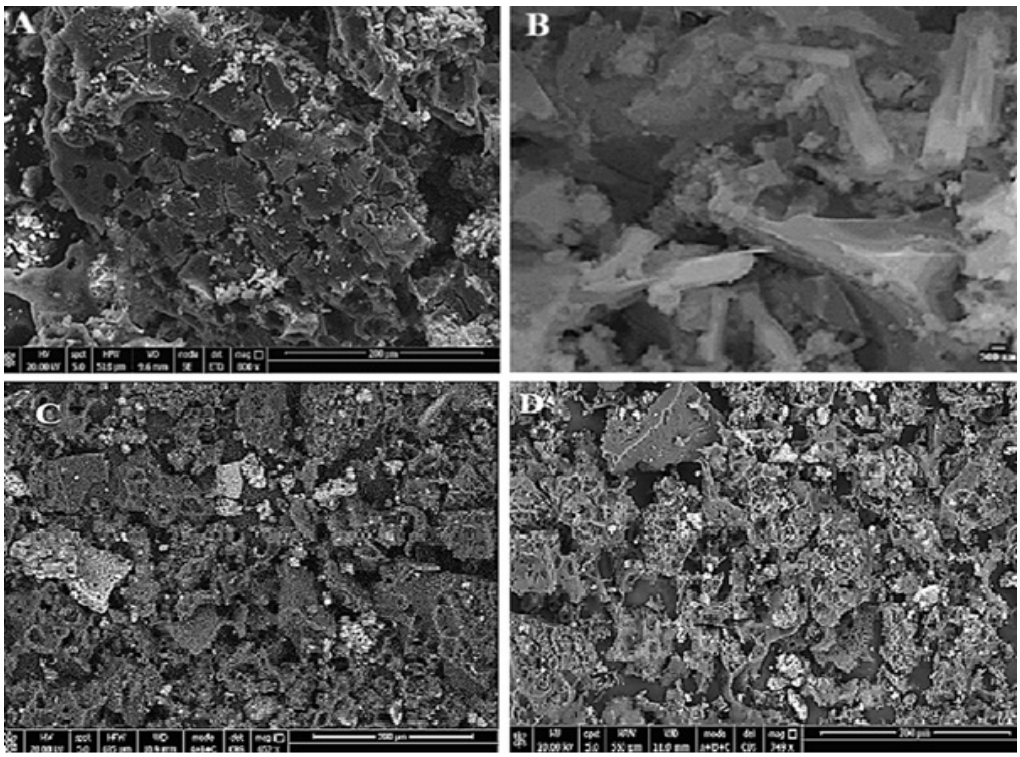

Fig. 3. SEM images of (A, B) ACs, (C) ACs after TGA, and (D) ACs after MB adsorption

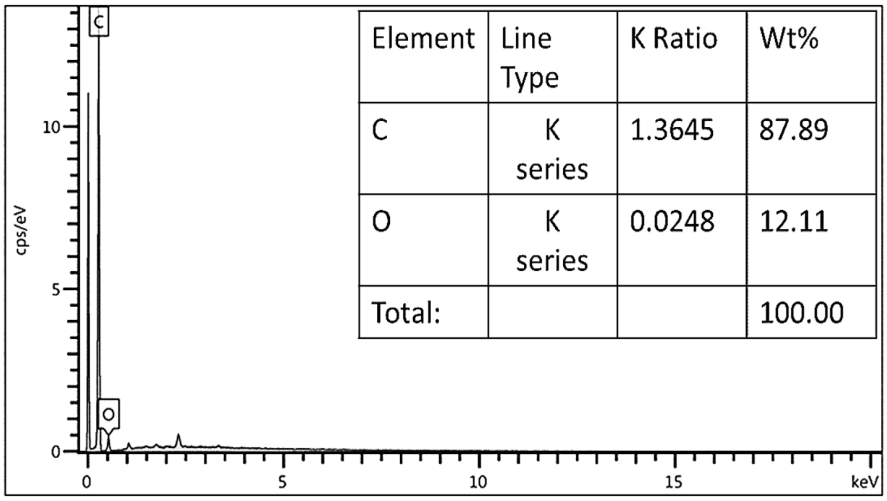

Element	Line Type	K Ratio	Wt%
C	K series	1.3645	87.89
O	K series	0.0248	12.11
Total:			100.00

Fig. 4. EDS for ACs

surface during the activation process [41]. The temperature was maintained at 410 °C for 1 hour to ensure sufficient contact time between the KOH and the biomass. The presence of small-diameter carbon rods (*ca*. 800 nm) increases the exposed surface area. This is another factor that increases adsorption and decreases the time required for MB dye uptake. EDX in Figure 4 shows that the ACs had high purity, with only carbon and oxygen atoms present in the final product, at 87.89% and 12.11%, respectively. The purity of activated carbon is an essential factor in its use across different applications. It is clear from Figure 5A that the AC's pore structure is destroyed after being heated to 800 °C by TGA. This could be due to the oxidation of biomass at high temperatures, which converts some of its carbon structure to ash. This is another indicator of the validity of carbonizing pumpkin seeds with 1.5 w/w KOH at 650 °C. Figure 5A displays the ACs after MB adsorption, revealing a distinct distribution of MB molecules in the accessible pore regions of the ACs' surface. Figure 5A shows significant weight loss in ACs from 25 °C to 150 °C, with approximately 10% mass loss attributed to water loss in various forms [42]. A slight mass loss occurs up to 650 °C, exceeding 200 °C, with about 3% loss. This behavior is consistent with the slow decomposition of biomass, which involves

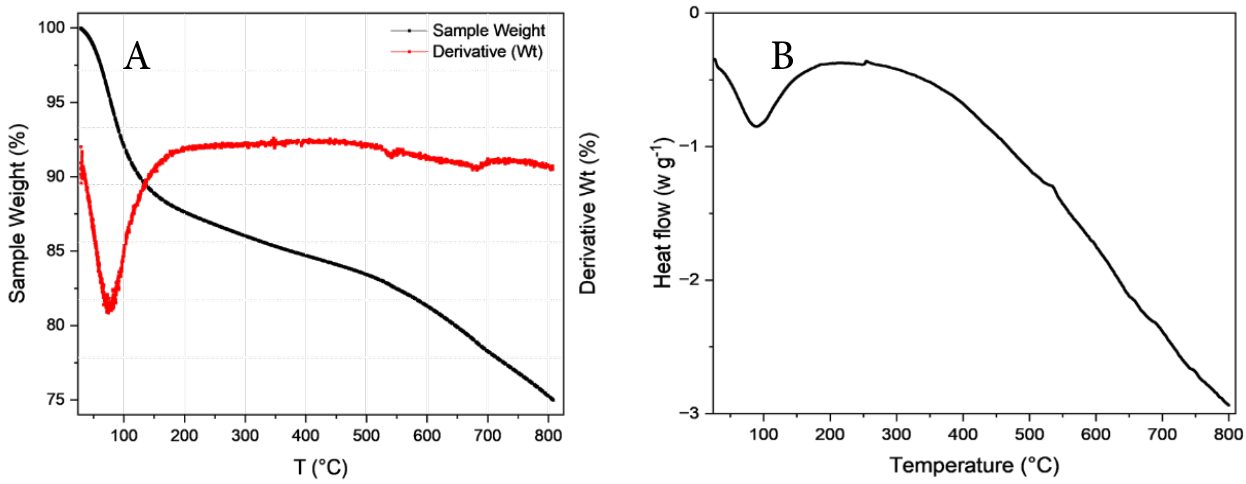

Fig. 5. A) TGA and B) DSC heating curves for AC

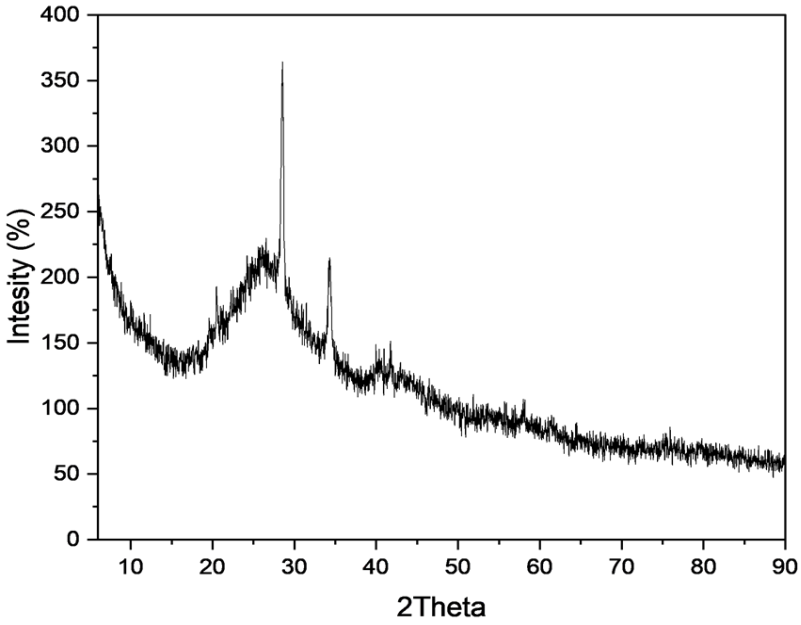

Fig. 6. XRD graphs for ACs

the formation of a carbonaceous skeleton and the recombination of structural components, the main sources of carbon. After 650 °C, ACs undergo significant weight loss, which can result in the conversion of carbon particles to CO and/or CO_2 [43]. This confirms the assumption that the optimal temperature for producing ACs from pumpkin seeds is 650°C, as it prevents substantial biomass loss and reduces energy consumption. The DSC graph in Figure 5B clearly shows a significant shift of the AC's endothermic peak toward higher temperatures. This may be related to the AC's superior thermal conductivity and rich pore structure. It is also typically possible to attribute the endothermic behavior to burn-off at high temperatures, which essentially fractures the carbon skeleton [44].

X-ray diffraction was used to confirm the crystallographic structures of the ACs, and the resulting patterns are shown in Figure 6. The broad peak indicates that ACs have an amorphous structure, the sharp peak at 2θ=~27° is in good agreement with the previously reported crystalline graphite[45]. Another peak, located at roughly 43°, is ascribed to the turbostratic nature of the carbons. XRD analysis indicates that our prepared ACs have some graphite with a crystalline structure[46]. This is also supported by the SEM image in Figure 3, which shows some rods of different sizes.

3.2. Adsorption Study

3.2.1.Effect of the AC amount

Figure 7 shows the effect of the amount of ACs on MB adsorption. Four different AC weights (0.01, 0.02, 0.04, and 0.06 g) were used to study the removal of MB (100 mL and 20 mg L^{-1}) within 5 min at 293 °K. It was observed that even a small amount of ACs (0.01 g) is sufficient to effectively eliminate more than 78% of the MB at 5.0 min. Furthermore, an increase in AC weight results in a slight increase in adsorption capacity, reaching 99% with 0.06 g of AC. This demonstrates the reliability of AC as a vital adsorbent for organic pollutants like MB in a liquid medium.

3.2.2.Effect of contact time

Another crucial aspect of the adsorption process is the investigation of the impact of the contact time between the AC and the dye. The outcome of contact time on the MB uptake by 0.05 mg of ACs at a fixed concentration (20 mg L^{-1}) and temperature of 293 °K is shown in Figure 8. It is clear that rapid adsorption occurs on the ACs, reaching 78%

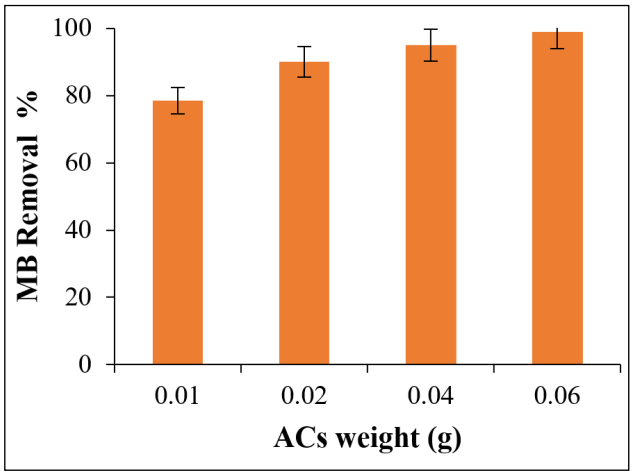

Fig. 7. Effect of AC amount on the MB removal

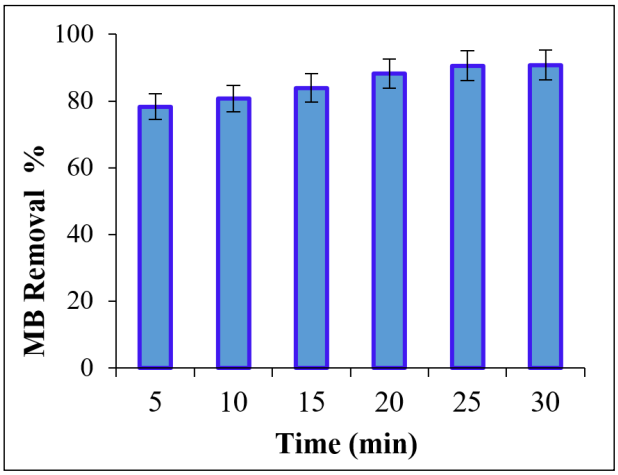

Fig. 8. Effect of contact time on the MB removal

in a short time (5 min), and the adsorption reaches 90% after 25 min. Thus, increasing the contact time beyond 25 minutes shows no significant improvement in MB adsorption, and the removal has reached equilibrium.

3.2.3.Effect of MB concentration

The impact of the concentration of MB on the adsorption process at a constant temperature of 20 °C and a weight of ACs of 0.05 g is shown in Figure 9. The figure shows that increasing the initial concentration of MB reduces the percentage removal: 99.5% at 5 mg L^{-1} and 75% at 30 mg L^{-1}. This is because the active sites on the ACs are limited. As a result, increasing the initial concentration does not significantly enhance MB removal; instead, the percentage of MB removal decreases linearly with the initial concentration.

3.2.4.Effect of temperature

The effect of temperature on adsorption is shown in Figure 10. The increase in temperature negatively affects MB adsorption on the ACs. It is not a significant effect: the removal of MB decreases by ~2.5% as the temperature increases from 293 °K to 333 °K. This is due to the desorption of MB, which chemically adsorbs on the ACs.

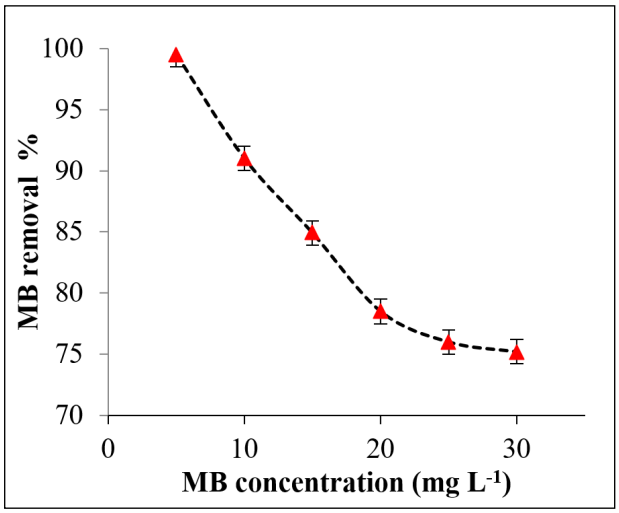

Fig. 9. Effect of MB concentration

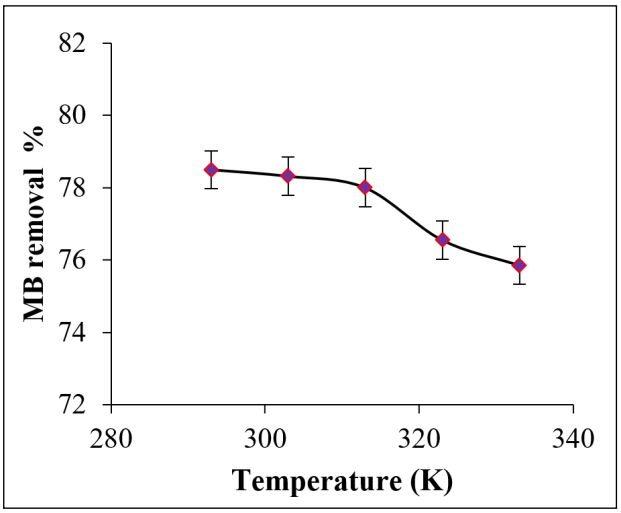

Fig. 10. Effect of temperature

3.2.5.Effect of media nature

Over 5 min, with an initial MB concentration of 20 mg L^{-1}, the effect of pH on MB removal was investigated in basic, neutral, and acidic media. Figure 11 shows a strong relationship between pH and MB removal. As predicted, the cationic dye was more effectively adsorbed in an alkaline environment compared to an acidic one. We found that increasing the media pH from 3 to 10 increased MB removal from 70% to 89%.

3.3. Isotherm model

The Freundlich isotherm is used to fit the MB experimental data using Equation 4 [47,48]. The relation between ln q_e and ln C_e is plotted, where the Freundlich constants (Kf and n) were calculated from the slope and the intercept, respectively, as summarized in Table 1. Figure 12 shows a non-linear relationship between ln q_e and ln C_e, indicating that the Freundlich isotherm does not apply to MB adsorption on the ACs. The values of K_f and n are 39.165 and -7.788, respectively, as shown in Table 1.

The results of MB adsorption were used to fit the Temkin isotherm using Equation 5. The relationship between qe and ln Ce is plotted, and the slope and intercept were used to calculate the values of K_T and Temkin's constant, B_T [48,49]. From Figure 13, it was found that there is a non-linear relationship between qe and ln (Ce), indicating that the Temkin isotherm does not apply to the adsorption of the dye on the ACs. The values of the constants B_T and K_T are -5.4216 and 0.001, respectively (Table 1).

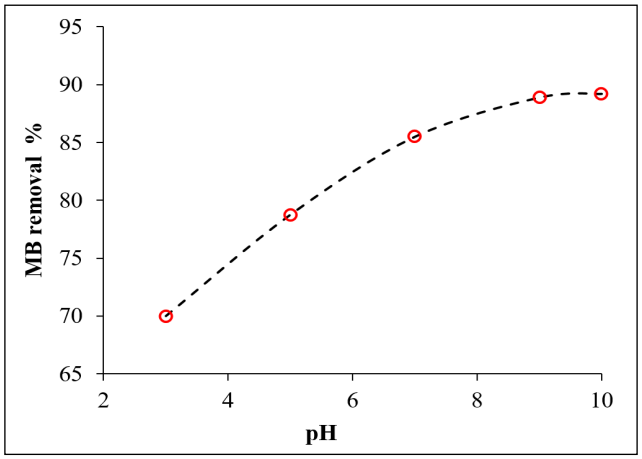

Fig. 11. Effect of pH on MB removal

Table 1. Values of Adsorption isotherm parameters

Isotherm	Parameters	Values
Langmuir	q_e	-0.4676
	q_{max}	28.9017
	b	-2.6615
	R^2	0.9985
Freundlich	n	-7.7880
	K_F	39.1650
	R^2	0.9878
Temkin	b_T	-5.4216
	R^2	0.9867

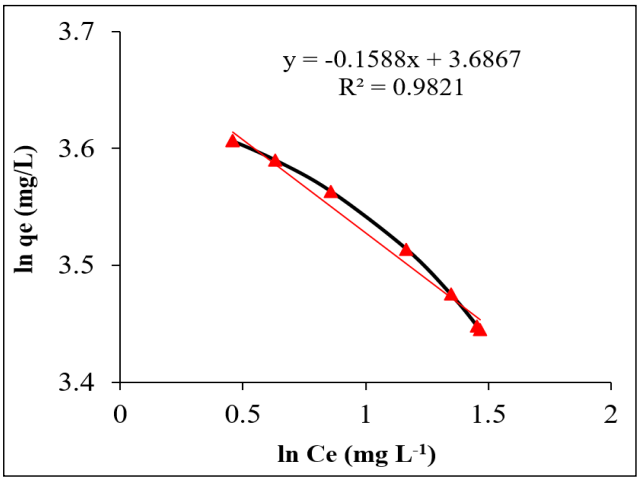

Fig. 12. Freundlich isotherm model

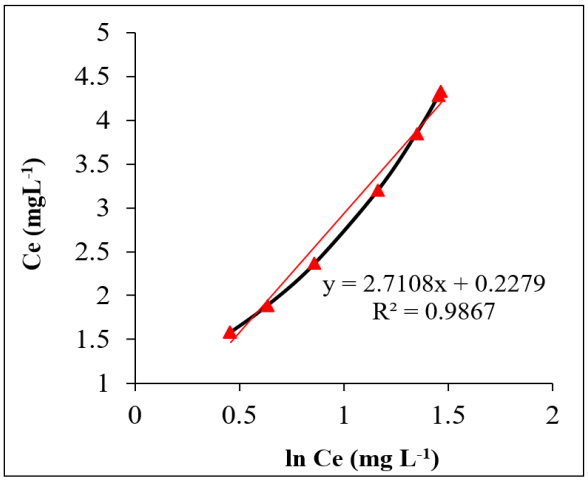

Fig. 13. The Temkin isotherm model

$$\log q_e = \log K_f + \frac{1}{n} \log C_e$$

(Eq.4)

$$q_e = B_T \, In \, K_T + B_T \, In \, C_e$$

(Eq. 5)

Where T is the absolute temperature (K), R is the gas constant (8.314 J $mol^{-1}K^{-1}$), and b is a constant related to the heat of adsorption (J mol^{-1}). K_T (mg L^{-1}) is the equilibrium binding constant, which indicates the maximum binding energy. B_T is a constant related to the differential surface capacitance of dye adsorption per unit bonding energy [48,49].

The Langmuir isotherm is essential for discussing adsorption systems based on the single-layer adsorption model. This means the energy on the surface of the activated carbon is evenly distributed, and the temperature remains constant. It also indicates the maximum capacity (q_{max}) of activated carbon[47–49]. According to Equation 6, a straight line with slope ($1/q_{max}$) and intercept ($1/b\,q_{max}$) can be obtained by plotting Ce/qe against Ce. It would then be possible to derive the values for b and q_{max}.

$$C_e/q_e = 1/(b * q_{max}) + (1/q_{max}) * C_e$$

(Eq. 6)

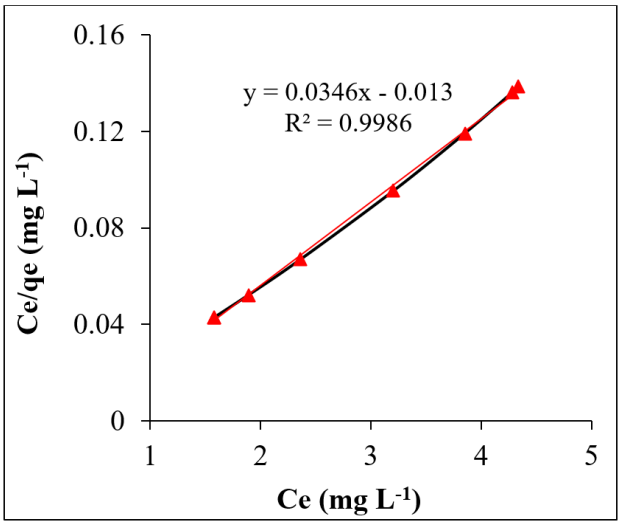

Fig. 14. Langmuir isotherm model

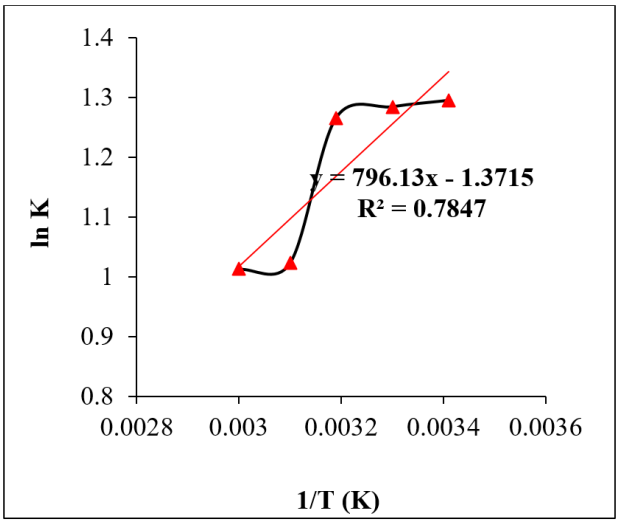

Fig. 15. The thermodynamic isotherm of MB

Table 2. Thermodynamic parameters of MB adsorption on ACs

Temperature °K	ΔH (KJ mol^{-1})	ΔS° (JK^{-1} mol^{-1})	ΔG° (KJmol^{-1})
293	6.640-	-11.894	-3.155
303		-11.235	-3.236
313		-10.691	-3.294
323		-12.053	-2.747
333		-11.521	-2.803

Where b is a factor related to the connection force between the dye and the adsorbent surface; q_{max} is the maximum theoretical adsorbent capacity (mg g^{-1}). Figure 14 shows that the Langmuir isotherm fits perfectly with the experimental data for MB dye adsorption. Since it gave the best linear relationship with a correlation coefficient (R) of 0.998 and q_{max} of -0.3757. As a result, it is possible to conclude that MB adsorption on the ACs occurs in a monolayer [47,48]. The thermodynamic variables of MB adsorption on the surface of ACs at various temperatures (293, 303, 308, 313, and 323 °K) were calculated using Equations 7-10. The thermodynamic isotherm of MB removal from water was shown in Figure 15 (t = 5 min, dose = 0.05 g, MB = 20 mg L^{-1}).

$$\ln K = \ln K_o - \frac{\Delta H}{RT} \quad \text{(Eq.7)}$$

$$\Delta G^o = -RT \ln K \quad \text{(Eq.8)}$$

$$\Delta G^o = \Delta H - T\Delta S^o \quad \text{(Eq.9)}$$

$$\Delta S^o = \frac{\Delta H - \Delta G^o}{T} \quad \text{(Eq.10)}$$

Where: K_o is the equilibrium adsorption coefficient, R is the gas constant, T is the temperature (K), and q_e is the quantity (mg L^{-1}) of MB adsorbed onto Ac at equilibrium[50–52]. Figure 15 shows ln K plotted vs. 1/T, which is used to determine the parameters ΔS and ΔH from the slope and intercept, respectively. Table 2 displays the parameters' respective values. It appears that the ΔG and ΔS have negative values while the ΔH has a positive value. These results indicate that the adsorption on ACs is spontaneous, with a high attraction between MB and the ACs surface, and the reaction is exothermic[50–52].

4. Conclusion

Pumpkin seeds were used as an abundant biomass source to produce ACs, with KOH as the activating agent. Such ACs show great potential for removing MB dye from aqueous solution, with sufficient performance. According to TGA results, 13% of the biomass is lost at ~100 °C due to relative humidity, and the optimal temperature for producing greater amounts of porous carbon is 650 °C. The SEM image reveals the AC surface porosity, thereby increasing the AC surface area. The methylene blue concentration was determined using a UV-Vis spectrophotometer with a standard curve (5–25 mg L^{-1}), and the limits of detection and quantification were 0.1027 and 0.3424 mg L^{-1}, respectively. The results of the adsorption process showed that ACs could be active and rapidly adsorbed at 293 °K. The isotherm study shows that MB adsorption on the ACs occurs in a monolayer, follows the Langmuir model, and is chemically absorbed.

5. Acknowledgement

We thank the University of Anbar, represented by the College of Science and the College of Applied Sciences-Hit, and the University of Fallujah/ College of Applied Sciences. We also thank the service research laboratory in the Department of Chemistry at the College of Science/ the University of Anbar.

6. References

[1] B.M. Hussien, M.A. Rabeea, M.M. Farhan, B. Muhie, M. Ayesh, H. Naji, Characterization and behavior of hydrogen sulfide plumes released from active sulfide-tar springs, Hit-Iraq, Atmos. Pollut. Res., 11 (2020) 894–902. https://doi.org/10.1016/j.apr.2020.02.001

[2] B.M. Hussien, M.A. Rabeea, H.N. Mukhlif, Estimation of corrosion and encrustation from groundwater chemistry of the aquifers: A case study of Al Hammad zone, Environ. Nanotechnology, Monit. Manag., 14 (2020) 100334. https://doi.org/10.1016/j.enmm.2020.100334

[3] A.S. Al-Rawi, A.M. Aljumialy, W.M. Saod, E.A. Al-Heety, Pollution level and sources of heavy metals in indoor dust from college of science, University of Anbar Campus, Iraq, IOP Conf. Ser. Earth Environ. Sci., 1300 (2024) 012019. https://doi.org/10.1088/1755-1315/1300/1/012019

[4] A.M. Aljumialy, A.S. Al-Rawi, W.M. Saod, E.A. Al-Heety, Ecological and health risk assessment of heavy metals in interior dust from college campus, Anal. Sci., 40 (2024) 1919-1926. https://doi.org/10.1007/s44211-024-00627-2

[5] M.A. Rabeea, A.S. Al-Rawi, O.J. Mohammad, B.M. Hussien, The residual effect of fish farms on the water quality of the Euphrates River, Iraq, Egypt. J. Aquat. Biol. Fish., 24 (2020) 549–561. https://doi.org/10.21608/EJABF.2020.102577

[6] A.T. Mohammed, A.M. Salman, O. Al-Muhandis, Determination of the optimum conditions for the recovery of silver from photographic fixer solutions used in hospitals and clinics at Anbar, Iraq, Asian J. Chem., 24 (2012) 5922–5926. https://asianpubs.org/index.php/ajchem/index

[7] I.A. Mawlood, W.M. Saod, A.S. Al-Rawi, A.M. Aljumialy, N. Hilal, Characterization and use of activated carbon synthesized from sunflower seed shell in the removal of Pb(II), Cd(II), and Cr(III) ions from aqueous solution, Environ. Monit. Assess., 196 (2024) 364. https://doi.org/10.1007/s10661-024-12525-1

[8] K. Watson, M.J. Farré, N. Knight, Strategies for the removal of halides from drinking water sources, and their applicability in disinfection by-product minimisation: A critical review, J. Environ. Manage., 110 (2012) 276–298. https://doi.org/10.1016/j.jenvman.2012.05.023

[9] M.A. Rabeea, T.A. Zaidan, A.J.R. Al-Heety, A.S. Al-Rawi, M. Elhag, Impact of municipal wastewater and sulfur springs on the physicochemical properties of the Euphrates River, Western Iraq, Desalin. Water Treat., 253 (2022) 63–77. https://doi.org/10.5004/dwt.2022.28292

[10] M.A. Rabeea, M.N. Owaid, A.A. Aziz, M.S. Jameel, M.A. Dheyab, Mycosynthesis of gold nanoparticles using the extract of Flammulina velutipes, Physalacriaceae, and their efficacy for decolorization of methylene blue, J. Environ. Chem. Eng., 8 (2020) 103841. https://doi.org/10.1016/j.jece.2020.103841

[11] M.A. Dheyab, M.N. Owaid, M.A. Rabeea, A.A. Aziz, M.S. Jameel, Mycosynthesis of gold nanoparticles by the Portabello mushroom extract, Agaricaceae, and their efficacy for decolorization of Azo dye, Environ. Nanotechnol. Monit. Manag., 14 (2020) 100312. https://doi.org/10.1016/j.enmm.2020.100312

[12] S.Y. Abdul-Hadi, M.N. Owaid, M.A. Rabeea, A. Abdul Aziz, M.S. Jameel, Rapid mycosynthesis and characterization of phenols-capped crystal gold nanoparticles from Ganoderma applanatum, Ganodermataceae,

Biocatal. Agric. Biotechnol., 27 (2020) 101683.
https://doi.org/10.1016/j.bcab.2020.101683

[13] M.A. Rabeea, M.N. Owaid, R.F. Muslim, Synthesis and characterization of silver nanoparticles by natural organic compounds extracted from eucalyptus leaves and their role in the catalytic degradation of methylene blue dye, Songklanakarin J. Sci. Technol., 43 (2021) 14–23.
https://doi.org/10.14456/sjst-psu.2021.3

[14] L. Borah, M. Goswami, P. Phukan, Adsorption of methylene blue and eosin yellow using porous carbon prepared from tea waste: Adsorption equilibrium, kinetics and thermodynamics study, J. Environ. Chem. Eng., 3 (2015) 1018–1028.
https://doi.org/10.1016/j.jece.2015.02.013

[15] Z. Esvandi, R. Foroutan, S.J. Peighambardoust, A. Akbari, B. Ramavandi, Uptake of anionic and cationic dyes from water using natural clay and clay/starch/MnFe2O4 magnetic nanocomposite, Surf. Interfaces, 21 (2020) 100754.
https://doi.org/10.1016/j.surfin.2020.100754

[16] M.A. Rabeea, R.F. Muslim, A.A. Younis, Preparation activated carbon from biji refinery asphalt treated with sulfur and waste polymers, Int. J. Appl. Eng. Res., 12 (2017) 14783–14788.
https://doi.org/10.13140/RG.2.2.28076.72329

[17] R.F. Muslim, M.A. Rabeea, T.A. Zaidan, Properties improvement of activated carbon prepared from hit natural asphalt by phenol formaldehyde polymer waste, Res. J. Pharm. Technol., 12 (2019) 2955–2958.
https://doi.org/10.5958/0974-360x.2019.00497.9

[18] J. Rakhtshah, H. Shirkhanloo, N. Esmaeil, A rapid extraction of toxic styrene from water and wastewater samples based on hydroxyethyl methylimidazolium tetrafluoroborate immobilized on MWCNTs by ultra-assisted dispersive cyclic conjugation-micro-solid phase extraction, Microchem. J., 170 (2021) 106759.
https://doi.org/10.1016/j.microc.2021.106759

[19] F.F. Ali, A.S. Al-Rawi, A.M. Aljumialy, Limestone residues of sculpting factories utilization as sorbent for removing Pb (II) ion from aqueous solution, Results Chem., 4 (2022) 100621.
https://doi.org/10.1016/j.rechem.2022.100621

[20] S. A. H. Mirzahosseini, S. A. Moussavi-Najarkola, H. Farahani, the evaluation and determination of heavy metals pollution in edible vegetables, water, and soil in the south of Tehran province by GIS, Arch. Environ. Prot., 41 (2015) 63-72.
https://doi.org/10.1515/aep-2015-0020

[21] F.F. Ali, A.S. Al-Rawi, A.M. Aljumialy, M.O. Ezzat, Dolomite utilization for removal of Zn2+ and Cu2+ ions from wastewater before determination by flame atomic absorption spectroscopy, Anal. Methods Environ. Chem. J., 7 (2024) 74–88.
https://doi.org/10.24200/amecj.v7.i02.311

[22] W.M. Saod, I.W. Oliver, D.F. Thompson, A. Contini, V. Zholobenko, Zinc oxide–mesoporous silica nanocomposite: preparation, characterisation and application in water treatment for lead, cadmium and chromium removal, Int. J. Environ. Anal. Chem., 104 (2023) 9772–9784.
https://doi.org/10.1080/03067319.2023.2246016

[23] W.M. Saod, I.W. Oliver, D.F. Thompson, S. Holborn, A. Contini, V. Zholobenko, Magnesium oxide loaded mesoporous silica: Synthesis, characterisation and use in removing lead and cadmium from water supplies, Environ. Nanotechnol. Monit. Manag., 20 (2023) 100817.
https://doi.org/10.1016/j.enmm.2023.100817

[24] A.S. Al-Rawi, I.K.I. Al-Khateeb, T.A. Zaidan, Nanocellulose acetate membranes: Preparation and application, Environ. Nanotechnol. Monit. Manag., 16 (2021) 100529.
https://doi.org/10.1016/J.ENMM.2021.100529

[25] S. Teimoori, H. Shirkhanloo, A.H. Hassani, M. Panahi, N. Mansouri, Rapid extraction of BTEX in water and milk samples based on functionalized multi-walled carbon nanotubes by dispersive homogenized-

micro-solid phase extraction, Food Chem., 421 (2023) 136229.
https://doi.org/10.1016/J.FOODCHEM.2023.136229

[26] A. Faghihi-Zarandi, J. Rakhtshah, B. Bahrami Yarahmadi, A rapid removal of xylene vapor from environmental air based on bismuth oxide coupled to heterogeneous graphene/ graphene oxide by UV photo-catalectic degradation-adsorption procedure, J. Environ. Chem. Eng., 8 (2020) 104193.
https://doi.org/10.1016/J.JECE.2020.104193

[27] R. Ashouri, S.A.H. Mirzahosseini, A. Rashidi, N. Mansouri, Synthesis of carbon quantum dots from olive stones for efficient adsorption of benzene from the ambient air, J. Nanostructures, 11 (2021) 480–497.
https://doi.org/10.22052/JNS.2021.03.007

[28] S. Teimoori, A.H. Hassani, M. Panahi, N. Mansouri, An immobilization of aminopropyl trimethoxysilane-phenanthrene carbaldehyde on graphene oxide for toluene extraction and separation in water samples, Chemosphere, 316 (2023) 137800.
https://doi.org/10.1016/J.CHEMOSPHERE.2023.137800

[29] F. Golbabaei, A. Vahid, A. Faghihi Zarandi, A novel nano-palladium embedded on the mesoporous silica nanoparticles for mercury vapor removal from air by the gas field separation consolidation process, Appl. Nanosci., 12 (2022) 1667-1682.
https://doi.org/10.1007/s13204-022-02366-0

[30] L.Z. Lee, M.A. Ahmad Zaini, One-step $ZnCl_2$/ $FeCl_3$ composites preparation of magnetic activated carbon for effective adsorption of rhodamine B dye, Toxin Rev., 41 (2022) 64–81.
https://doi.org/10.1080/15569543.2020.1837172

[31] R. Ashouri, H. Shirkhanloo, A.M. Rashidi, S.A.H. Mirzahosseini, N. Mansouri, Dynamic and static removal of benzene from air based on task-specific ionic liquid coated on MWCNTs by sorbent tube-headspace solid-phase extraction procedure, Int. J. Environ. Sci. Technol., 18 (2021) 2377–2390.
https://doi.org/10.1007/S13762-020-02995-4

[32] M.M. Asl, N. Mansouri, S.A.R.H.S. Mirzahosseini, F. Atabi, Functionalized Graphene Oxide with Bismuth and Titanium Oxide Nanoparticles for Efficiently Removing Formaldehyde from the Air by Photocatalytic Degradation–Adsorption Process, J. Anal. Test., 7 (2023) 444–458.
https://doi.org/10.1007/S41664-023-00272-0

[33] M. Mohammadi Asl, N. Mansouri, S.A.R. Haji Seyed Mirzahosseini, F. Atabi, Simultaneity comparative evaluation of toluene removal from the air by adsorption and UV semi-degradation-based adsorption procedure, Int. J. Environ. Sci. Technol., 21 (2024) 6677–6694.
https://doi.org/10.1007/S13762-024-05503-0

[34] S. Teimoori, H. Shirkhanloo, A.H. Hassani, M. Panahi, N. Mansouri, New extraction of toluene from water samples based on nano-carbon structure before determination by gas chromatography, Int. J. Environ. Sci. Technol., 20 (2023) 6589–6608.
https://doi.org/10.1007/S13762-023-04906-9

[35] Z. Heidarinejad, M.H. Dehghani, M. Heidari, G. Javedan, I. Ali, M. Sillanpää, Methods for preparation and activation of activated carbon: a review, Environ. Chem. Lett., 18 (2020) 393–415.
https://doi.org/10.1007/s10311-019-00955-0

[36] A. Faghihi-Zarandi, C. Jamshidzadeh, A new method for removal of hazardous toluene vapor from air based on ionic liquid-phase adsorbent, Int. J. Environ. Sci. Technol. 16 (2019) 2797–2808.
https://doi.org/10.1007/S13762-018-1975-5

[37] X. Ji, B. Peng, H. Ding, B. Cui, H. Nie, Y. Yan, Purification, Structure and biological activity of pumpkin polysaccharides: A review, Food Rev. Int., 39 (2023) 307–319.
https://doi.org/10.1080/87559129.2021.1904973

[38] J.M. Dotto, J.S. Chacha, The potential of pumpkin seeds as a functional food ingredient: A review: Biofunctional ingredients of pumpkin seeds, Sci. Afr., 10 (2020) e00575.
https://doi.org/10.1016/j.sciaf.2020.e00575

[39] J. Huang, Z. Wang, Y. Qiao, B. Wang, Y. Yu, M. Xu, Transformation of nitrogen during hydrothermal carbonization of sewage sludge: Effects of temperature and Na/Ca acetates addition, Proc. Combust. Inst., 38 (2021) 4335–4344. https://doi.org/10.1016/j.proci.2020.06.075

[40] M.A. Rabeea, T.A. Zaidan, A.H. Ayfan, A.A. Younis, High porosity activated carbon synthesis using asphaltene particles, Carbon Lett., 30 (2020) 199–205. https://doi.org/10.1007/s42823-019-00086-0

[41] J.H. Kim, S.Y. Hwang, J.E. Park, G.B. Lee, H. Kim, S. Kim, B.U. Hong, Impact of the oxygen functional group of nitric acid-treated activated carbon on KOH activation reaction, Carbon Lett., 29 (2019) 281–287. https://doi.org/10.1007/s42823-019-00024-0

[42] J. Montalvo Andia, A. Larrea, J. Salcedo, J. Reyes, L. Lopez, L. Yokoyama, Synthesis and characterization of chemically activated carbon from Passiflora ligularis, Inga feuilleei and native plants of South America, J. Environ. Chem. Eng., 8 (2020) 103892. https://doi.org/10.1016/j.jece.2020.103892

[43] R. Maniarasu, S.K. Rathore, S. Murugan, Preparation, characterization, and performance of activated carbon for CO2 adsorption from CI engine exhaust, Greenh. Gases Sci. Technol., 12 (2022) 284–304. https://doi.org/10.1002/ghg.2145

[44] R.A. Shawabkeh, Z. Aslam, I.A. Hussien, Thermochemical treatment of fly ash for synthesis of mesoporous activated carbon, J. Therm. Anal. Calorim., 122 (2015) 1191–1201. https://doi.org/10.1007/s10973-015-4964-7

[45] A.H. Jawad, K. Ismail, M.A.M. Ishak, L.D. Wilson, Conversion of Malaysian low-rank coal to mesoporous activated carbon: Structure characterization and adsorption properties, Chinese J. Chem. Eng., 27 (2019) 1716–1727. https://doi.org/10.1016/j.cjche.2018.12.006

[46] V.A. Sugiawati, F. Vacandio, N. Yitzhack, Y. Ein-Eli, T. Djenizian, Direct pre-lithiation of electropolymerized carbon nanotubes for enhanced cycling performance of flexible li-ion micro-batteries, Polymers (Basel), 12 (2020) 406. https://doi.org/10.3390/polym12020406

[47] S. Sen Gupta, K.G. Bhattacharyya, Interaction of metal ions with clays: I. A case study with Pb (II), Appl. Clay Sci., 30 (2005) 199–208. https://doi.org/10.1016/j.clay.2005.03.008

[48] A.A. El-Bayaa, N.A. Badawy, E. Abd AlKhalik, Effect of ionic strength on the adsorption of copper and chromium ions by vermiculite pure clay mineral, J. Hazard. Mater., 170 (2009) 1204–1209. https://doi.org/10.1016/j.jhazmat.2009.05.100

[49] S. Mnasri-Ghnimi, N. Frini-Srasra, Removal of heavy metals from aqueous solutions by adsorption using single and mixed pillared clays, Appl. Clay Sci., 179 (2019) 105151. https://doi.org/10.1016/j.clay.2019.105151

[50] D.K. Mondal, B.K. Nandi, M.K. Purkait, Removal of mercury (II) from aqueous solution using bamboo leaf powder: equilibrium, thermodynamic and kinetic studies, J. Environ. Chem. Eng., 1 (2013) 891–898. https://doi.org/10.1016/j.jece.2013.07.034

[51] A.H. Jawad, A.S. Abdulhameed, Mesoporous Iraqi red kaolin clay as an efficient adsorbent for methylene blue dye: Adsorption kinetic, isotherm and mechanism study, Surf. Interfaces, 18 (2020) 100422. https://doi.org/10.1016/j.surfin.2019.100422

[52] T.C. Umeh, J.K. Nduka, K.G. Akpomie, Kinetics and isotherm modeling of Pb (II) and Cd (II) sequestration from polluted water onto tropical ultisol obtained from Enugu Nigeria, Appl. Water Sci., 11 (2021) 65. https://doi.org/10.1007/s13201-021-01402-8